

Toward Centimeter-Scale Human Activity Sensing with Wi-Fi Signals

Daqing Zhang, Hao Wang, and Dan Wu, Peking University

By enabling centimeter-scale human activity sensing with Wi-Fi signals, the Fresnel zone model could revolutionize wireless sensing and Internet of Things applications.

With wireless technologies' rapid development, the role of Wi-Fi RF signals has been extended from that of a sole communication medium to a nonintrusive environmental sensing tool.¹ In indoor environments, RF signals propagate in the wireless medium through multipaths, bouncing off different objects before arriving at a receiver and, hence, carrying information about the environment. By analyzing the received RF signal patterns and characteristics, we can detect human activities and behavioral statuses such as respiration rate, gestures, and falls—a process called contactless or device-free human sensing.

Combining wireless sensing and communication in a computing device has been a research goal for two decades, starting with the RADAR indoor localization system. Although most work has focused on human sensing using Wi-Fi-received signal strength (RSS), sensing applications have been limited because the multipaths cause unpredictable RSS fluctuations.¹ The situation has

changed now that physical-layer channel state information (CSI) is accessible on commodity Wi-Fi devices.²

CSI contains detailed phase and amplitude information about each subcarrier and can depict each subcarrier's propagation path; thus, a surge of recent research efforts in the Wi-Fi-based sensing field have exploited fine-grained CSI, enabling applications ranging from fall detection to vital-sign monitoring.^{3–6} Wi-Fi signals containing dozens of subcarriers are simultaneously affected by static objects and dynamic human activities in the environment; each subcarrier is affected differently by human activities such as gestures, falls, and respiration, making CSI-based signal analysis more precise, fine grained, and richer than RSS-based approaches that leverage only the aggregated signal strength. Whereas most current work has focused on Wi-Fi signals' variation patterns, there has been little exploration of the sensing limit and generic theory informing the design of Wi-Fi sensing systems.

In this article, we examine the basic theoretical foundation for RF-based sensing systems and shed light on



See www.computer.org/computer-multimedia for multimedia content related to this article.

the sensing limit of Wi-Fi RF signals. Specifically, we introduce the Fresnel zone model to the indoor environment, using it to depict RF signal-propagation properties and further develop techniques for indoor respiration detection and direction estimation using commodity Wi-Fi devices. We show that this model can enable centimeter-scale human activity recognition and potentially expand applications in areas such as healthcare, localization, and human-computer interaction into new territories.

EVOLUTION OF WI-FI RF-BASED SENSING THEORY

In a typical indoor environment, the receiver gets RF signals not only from the direct path—known as the line of sight (LoS)—but also from massive multipaths (non-LoS) caused by reflection, diffraction, and scattering.⁷ When a person is in the indoor environment, new paths will be diffracted and reflected from his or her body. The received signal is a linear combination of signals from all these paths. For a radio wave with wavelength λ traveling along a path of length d , its phase shifts $2\pi d/\lambda$. The received signal can then be expressed as the vector sum

$$\sum a_i e^{-iz\pi d_i/\lambda},$$

where i is the path number and a_i is the attenuation coefficient of each path. If the person is static in the environment, the received signal is almost stable; if the person moves, the received signal will keep changing. The key challenge here is correlating the waveforms of the received signal with specific human motions.

The early RF propagation model adopted for indoor localization was the path loss model,⁷ in which the received signal amplitude's fluctuation due to human motion was attributed to path loss (attenuation) of the reflected signal;⁶ in other words, the reflected path length changed with the person's motion, leading to RSS fluctuation. However, it is difficult to quantify each path in indoor, multipath, rich environments.⁷ Thus, most early CSI-based human-sensing work resorted to extensive empirical experiments and statistical analysis of the Wi-Fi signals.^{3,4,8}

The recently proposed interference-based propagation model divides all indoor multipaths into static and dynamic paths; as the path length of the dynamic reflected signal changes, the phases of the reflected signals change.⁹

The received signal's fluctuation is attributed to the interference of the dynamic signals and the superimposed static signals. In this way, a quantitative relationship between CSI dynamics and human movement speed is established.

WE CAN CAPTURE SUBTLE BODY DISPLACEMENT ON THE RECEIVING RF SIGNAL AT THE GRANULARITY OF SUBWAVELENGTHS.

However, it is still difficult to correlate the CSI waveform to human motions in geometrical space.

Initially used in outdoor environments, the Fresnel zone model is a propagation theory that calculates reflection and diffraction loss between transmitters and receivers in geometrical space.¹⁰ See the sidebar for a brief overview of the model's origins.

FRESNEL ZONE MODEL AND PROPERTIES

Fresnel zones refer to the series of concentric ellipsoids of alternating strength that are caused by a light or radio wave following multiple paths as it propagates in free space, resulting in constructive and destructive interference as the different-length paths go in and out of phase. Assuming P_1 and P_2 are two radio transceivers (see Figure 1a), the Fresnel zones are the concentric ellipsoids with foci in the pair of transceivers. For a given radio wavelength λ , Fresnel zones containing n ellipsoids can be constructed by ensuring that

$$|P_1 Q_n| + |Q_n P_2| - |P_1 P_2| = n\lambda/2,$$

where Q_n is a point in the n th ellipse. There are an infinite number of Fresnel zones. The innermost ellipsoid is defined as the first Fresnel zone, the elliptical annuli between the first and second ellipsoids is defined as the second Fresnel zone, and the n th Fresnel zone corresponds to the elliptical annuli between the $n-1$ th and n th ellipsoids. Because the boundary between two adjacent Fresnel zones is an ellipsoid, the boundary of the n th Fresnel zone is defined as the ellipsoid between the n th and $n+1$ th Fresnel zones.

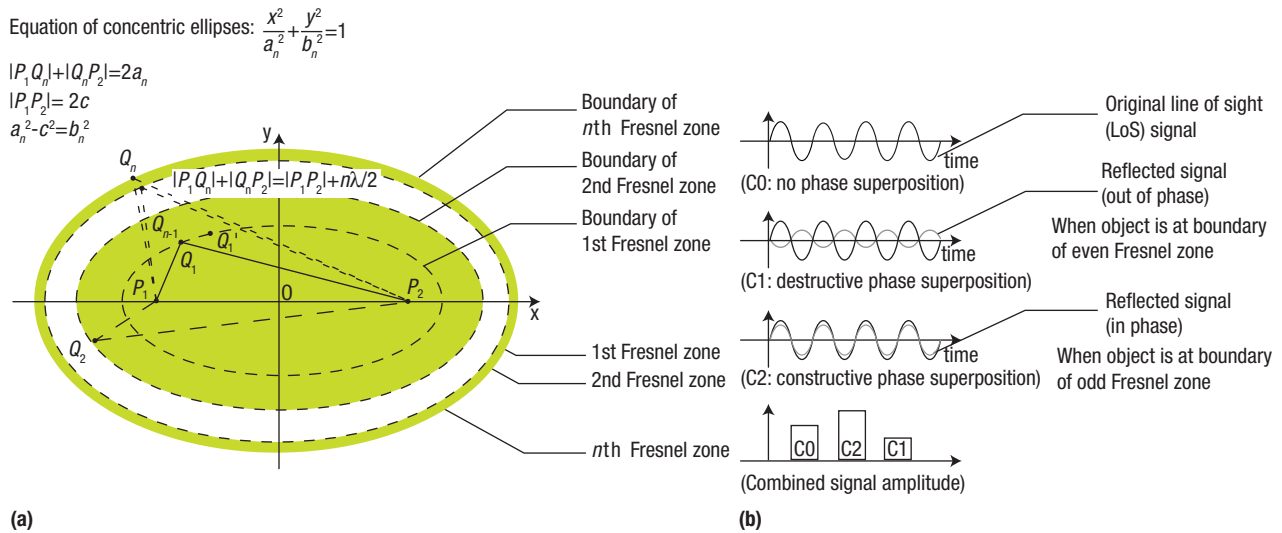


FIGURE 1. (a) Fresnel zones and (b) signal superposition. The Fresnel zones are the concentric ellipsoids with foci in a pair of transceivers, P_1 and P_2 .

How objects in Fresnel zones affect the received RF signal

When an object appears in the Fresnel zones in free space, the radio signal is viewed as traveling from the transmitter to the receiver via two paths: one that goes directly (the LoS path) and another that is reflected by the object (the reflected path). The two signals combine to create a superimposed signal at the receiver side. When a signal is reflected, the phase of the signal reverses and changes by π .⁷ If the two signals have a phase difference of 2π (in phase), they reinforce the signal strength; if the two signals have a phase difference of π (out of phase), they cancel each other and decrease the signal strength.

For example, assume that an object Q_1 appears at the first Fresnel zone boundary, as shown in Figure 1a. The reflected signal's path length ($|P_1Q_1P_2|$) is $\lambda/2$ longer than the LoS's, and the relative phase difference of signals between the two paths is π ; adding the phase shift π introduced by the reflection causes the two signals to be in the same phase, leading to constructive interference and a stronger superimposed received signal, as shown by C2 in Figure 1b. Similarly, an object located at the second Fresnel zone boundary creates destructive interference and a degraded received signal, as shown by C1 in Figure 1b. In short, at the boundary of an odd-numbered Fresnel zone, an object creates a reinforced signal; at an even-numbered zone's boundary, the object creates a degraded signal. This produces interleaved interference patterns.

We conducted indoor experiments with a pair of Wi-Fi transceivers and a metal cup to verify the Fresnel zones' existence and to show that the received signal varies as expected when an object moves across the zones. We set the Wi-Fi channel frequency to 5.24 GHz, and moved the cup 15 cm along three directions. The received signals recorded

show that the number and sequence of valleys and peaks generated by the moving cup match those of the Fresnel zones crossed.¹¹

Characterizing the received signal in a moving object's presence

As demonstrated in Figure 1a, suppose an object moves in the Fresnel zones from Q_1 to Q_n ; while the signal traveling via the LoS remains the same, the signal reflected by the object changes over time. As the length of the reflected path changes, the relative phase difference between the LoS signal and the reflected signal changes accordingly. Based on the interference analysis, the received signal will present peaks or valleys when the object crosses the boundary of the Fresnel zones. However, if the object moves along ellipses, the reflected signal path's length does not change and so the received signal remains the same.

To characterize the received signal in the presence of a moving object, we studied a typical setting, shown in Figure 2a, in which a transmitted signal arrives at the receiver by multiple paths. By dividing these paths into static and dynamic paths, the received signal $H(f,t)$ can be denoted as a phase vector:^{7,9}

$$H(f,t) = H_s(f) + H_d(f,t) = H_s(f) + a(f,t)e^{-j2\pi d(t)/\lambda},$$

where the static vector $H_s(f)$ is the sum of signals from static paths, and the dynamic vector $H_d(f,t)$ is introduced by the reflected signal from the moving object, as shown in Figure 2b. The reflected signal can be further represented by a vector, where $a(f,t)$ is the complex valued representation of amplitude and initial phase offset of the dynamic path, and $e^{-j2\pi d(t)/\lambda}$ is the phase shift along the dynamic path length $d(t)$. Apparently, when the length of the reflected

HISTORY OF THE FRESNEL ZONE MODEL

The Fresnel zone concept originated with Augustin Fresnel's early 19th-century research on light's interference and diffraction.¹ Fresnel's work revealed the physical properties of light when it travels from a source point to an observation point. Fresnel zones refer to the series of concentric ellipses with two foci corresponding to the source and observation points. Light waves traveling through the first Fresnel zone are all in phase, enhancing the light strength received at the observation point. Successive Fresnel zones alternately provide constructive and destructive interference to the received light at the observation point. The first mention of using the Fresnel zone concept with RF appeared in a 1936 US patent.^{2,3} Since then, the Fresnel zone model has found various practical applications ranging from microwave propagation in wireless links to wireless station placement to antenna design.⁴ Recent work applies the Fresnel–Kirchhoff knife-edge diffraction model with received signal strength for localization achieving meter-scale resolution.⁵ We, however, consider the reflection and frequency diversity

of the Wi-Fi RF signal in constructing the Fresnel zone model and reveal the signal-change pattern in each subcarrier caused by a person's movement. Thus, we can capture subtle body displacement on the receiving RF signal at the granularity of subwavelengths, pushing the sensing resolution to an unprecedented centimeter level.

References

1. F.A. Jenkins and H.E. White, *Fundamentals of Optics*, Tata McGraw-Hill Education, 1957.
2. G.C. Andre and H.D. Rene, *Directional Radio Transmission System*, US patent 2,043,347, Patent and Trademark Office, 1936.
3. J.C. Wiltse, "History and Evolution of Fresnel Zone Plate Antennas for Microwaves and Millimeter Waves," *Proc. IEEE Antennas and Propagation Society Int'l Symp.*, 1999, pp. 722–725.
4. H.D. Hristov, *Fresnel Zones in Wireless Links, Zone Plate Lenses and Antennas*, Artech House, 2010.
5. C. Liu et al., "RSS Distribution-Based Passive Localization and Its Application in Sensor Networks," *IEEE Trans. Wireless Communications*, vol. 15, no. 4, 2016, pp. 2883–2895.

signal changes by λ , its phase shifts 2π (rotates one round). Hence, the received signal $H(f,t)$ has a time-varying amplitude in a complex plane:

$$|H(f, \theta)|^2 = |H_s(f)|^2 + |H_d(f)|^2 + 2|H_s(f)||H_d(f)|\cos\theta, \quad (1)$$

where θ is the phase difference between the static vector $H_s(f)$ and dynamic vector $H_d(f)$. In particular, when the object moves a short distance, such as several wavelengths as shown in Figure 2c, it is safe to assume that the amplitude of the dynamic vector remains the same; that is, $H_d(f)$ is constant. This explains why the amplitude of the received signal looks like a sinusoidal wave when the object crosses several Fresnel zones. Specifically, the peaks appear when $\theta = 2\pi, 4\pi, \dots$ and the valleys appear when $\theta = 3\pi, 5\pi, \dots$, corresponding to the boundaries of the Fresnel zones.

In real environments, a single RF subcarrier corresponds to one set of Fresnel zones, even though multiple static signal paths are incurred by the surrounding static objects. As the generated Fresnel zones are determined by the aggregated signal vector of all static multipaths, the reflected signals are generally weaker than the LoS signal, making the

location and size of the Fresnel zones slightly different from the standard ones shown in Figure 1a. When there are multiple static objects and one moving object, as in Figure 2a, we use the aggregated signal vector of all static multipaths to generate the Fresnel zones and treat the moving object using Equation 1. When there are multiple moving objects in the environment, the Fresnel zone model is determined by the aggregated signal vector of all multipaths, which is dynamic and time varying. In this case, if the moving objects are small and far from the transceivers, the dynamic path signals usually have a negligible effect on the aggregated signal compared to the strong and static LoS signal; thus, we can still approximate the Fresnel zone model using the major static paths' signals. But if all the moving objects significantly affect the received signal compared to the LoS signal, the static Fresnel zone model might not analyze the signal-propagation properties correctly.

RF signal-propagation properties in the Fresnel zones

We can summarize the Wi-Fi RF signal-propagation properties in indoor space as follows:

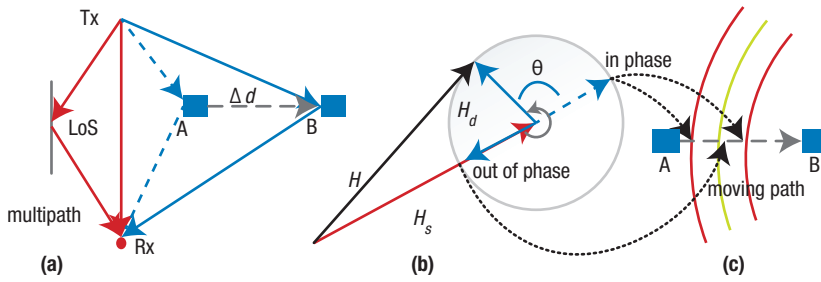


FIGURE 2. Linear superposition of multipath signals. (a) In a typical setting, a transmitted signal arrives at the receiver by multiple paths. (b) By dividing these paths into static and dynamic paths, the received signal $H(f,t)$ can be denoted as a phase vector: the static vector $H_s(f)$ is the sum of signals from static paths and the dynamic vector $H_d(f,t)$ is introduced by the reflected signal from the moving object. (c) When the reflected signal's length changes by λ , its phase shifts 2π (rotates one round). Hence, the received signal $H(f,t)$ has a time-varying amplitude in a complex plane: θ is the phase difference between the static vector $H_s(f)$ and dynamic vector $H_d(f)$. When the object moves a short distance, the amplitude of the dynamic vector remains the same; that is, $H_d(f)$ is constant.

- ▶ P1: Wi-Fi Fresnel zones take the shape of concentric ellipsoids with foci in a pair of transceivers.
- ▶ P2: When an object crosses a series of Fresnel zones, the received signal shows a continuous sinusoidal-like wave, with peaks and valleys generated by crossing the Fresnel zone boundaries.
- ▶ P3: A moving object usually produces a reflected signal with varying amplitude and phase. On a small moving scale, the reflected signal has a roughly fixed amplitude with varying phase affecting the received signal. On a large moving scale, the reflected signal experiences both phase change and amplitude attenuation caused by path loss.
- ▶ P4: If the reflected signal from a moving object changes the path length by one wavelength (for example, 5.725 cm for 5.24 GHz), its phase will undergo a 2π change, generating a complete sinusoidal cycle; if the reflected signal changes the path length such that it is shorter than one wavelength, the generated signal is a fragment of the sinusoidal cycle.

WI-FI MULTIFREQUENCY RF SIGNAL FRESNEL ZONE MODEL

The Wi-Fi 802.11n+ specification leverages an orthogonal frequency-division multiplexing (OFDM)-based transmission scheme that divides the whole bandwidth into multiple subcarriers with different frequencies. Multiple Fresnel zones are thus formed around the transmitter (Tx) and receiver (Rx) antennas according to their wavelengths.

Characterizing the relationship among multifrequency Fresnel zones

These multifrequency Fresnel zones share the same (or similar) foci and shape but slightly different sizes: a subcarrier with a shorter wavelength has smaller ellipsoids;

more specifically, for the inner Fresnel zones, the geometrical layouts from different subcarriers almost overlap with one another. The gap increases as the number of Fresnel zones increases (see Figure 3a), until the boundary of the $(i+1)$ th Fresnel zone with the smaller wavelength catches up with that of the i th Fresnel zone with the larger wavelength (see Figure 3b).

To quantify this difference, we define the angle θ between the static vector H_s and dynamic vector H_d in Figure 2b as the Fresnel phase; this difference can then be characterized by calculating the phase difference between the two Fresnel phases of two subcarriers with wavelength λ_1 and λ_2 as

$$\Delta\theta = 2\pi(d_1 - d_0)\Delta f/c, \quad (2)$$

where Δf is the frequency gap of the two subcarriers; c is the light speed in air; and d_0, d_1 are the direct path and reflected path, respectively. From Equation 2, we see that the difference is only relevant to the gap between two frequencies, not the carrier frequency itself; moreover, this difference has a linear relationship with the path-length difference between d_0 and d_1 for a given Δf .

Wi-Fi multifrequency RF signal propagation properties

We can summarize the Wi-Fi RF propagation properties in multiple frequencies as follows:

- ▶ P5: Because different subcarriers have different radio wavelengths, each subcarrier has its own Fresnel zones.
- ▶ P6: Inner Fresnel zones of different subcarriers almost overlap; however, the gap between two Fresnel zone boundaries keeps increasing in outer zones until one catches the next boundary of the other (see Figure 3a). In other words, in inner Fresnel zones there are big gaps between zone boundaries, but in outer zones those boundaries are evenly distributed.
- ▶ P7: The shape of the Fresnel zone of a subcarrier with a shorter wavelength is smaller than that of a subcarrier with a larger wavelength. So, for the k th Fresnel zone boundary, the Fresnel zone boundary

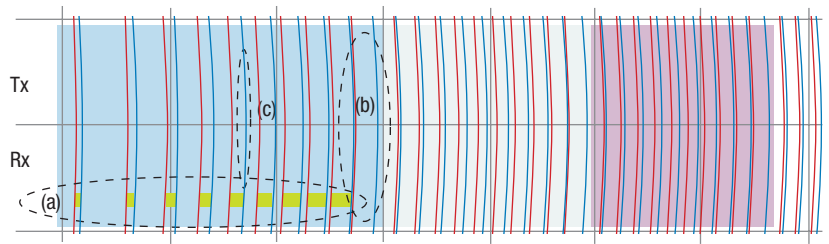


FIGURE 3. Geometrical relationship of two subcarriers' Fresnel zones: subcarrier with smaller wavelength (red) versus larger wavelength (blue). The subcarrier with the shorter wavelength has smaller ellipsoids. (a) The gap increases as the number of Fresnel zones increases, until (b) the boundary of the $(i+1)$ th Fresnel zone with the smaller wavelength catches up with that of the i th Fresnel zone with the larger wavelength. (c) Before reaching (b), this region contains two subcarriers with nearly equally spaced interleaved Fresnel zones. Rx: receiver; Tx: transmitter.

of a subcarrier with a shorter wavelength is located inside of the k th boundary of the subcarrier with the longer wavelength.

- **P8:** When multiple antennas are equipped and placed apart from one another in commodity Wi-Fi devices, the RF signal between each Rx-Tx pair creates its own Fresnel zones; thus, multiple pairs of Rx-Tx antennas create overlapping Fresnel zones.

APPLYING THE FRESNEL ZONE MODEL TO HUMAN SENSING

Here, we use two real applications to show how the Fresnel zone model can recognize micro and macro human activities. Specifically, we apply the model to inform where and why human respiration can be detected, demonstrating Wi-Fi signals' centimeter-scale human motion-detection capabilities.¹¹ We also utilize the model to accurately estimate walking direction indoors, demonstrating detection of decimeter-scale human motion.¹²

Human respiration rate detection

Respiration rate is an important vital sign that can indicate the progression of an illness and declines in health. Traditionally, monitoring vital signs requires patients to visit the hospital and wear dedicated sensors. For cost-effective and nonintrusive home monitoring systems, researchers have turned their attention to commodity Wi-Fi devices for contact-free vital sign measurement.^{4,5} However, sensing human respiration with Wi-Fi signals is challenging because it requires centimeter-scale detection accuracy; the received signal from such micro human activities is often so weak that it cannot be distinguished from environmental noises. Therefore, in actual implementation, users are requested to stay either between the LoS or very close to the transceivers. As previous work is based on purely empirical experiments—without a theoretical model to guide the system design—it fails to tell why and when subtle human movement can be detectable and thus resorts to trial and error. In our recent work, we analyzed the received signal fluctuation caused by the subtle chest displacement of respiration, and demonstrate when and why human respiration is detectable based on the Fresnel zone model.¹¹

Correlating subtle chest displacement to signal fluctuation. The mean displacement of chest movement for normal respiration is around 5 mm,¹³ so the path-length change caused by human respiration is smaller than a wavelength. According to P3, the received signal waveform caused by human respiration is only a fragment of the sinusoidal cycle. Specifically, the phase rotation θ caused by respiration in Figure 2b is only around 60° .¹¹

As one respiration cycle consists of an inhalation followed by a pause and an exhalation followed by another pause, and human respiration is usually periodical, then, according to Equation 1, the received signal also consists of four segments: a waveform generated by inhalation, a straight line caused by the pause after inhalation, a waveform generated by exhalation, and another straight line caused by the pause after exhalation. Given the 60° phase change θ that lies in the cycle of the cosine wave (see Figure 4a), both θ 's angle and position affect the shape of the signal waveform. To make respiration rate easy to extract correctly, the θ angle is expected to not only cover a large range but to also lie fully in the monotonically changing fragment of the cosine wave. In particular, the best choice for the cosine wave fragment of a fixed θ is centered around $\pi/2$ or $3\pi/2$, corresponding to the middle of each Fresnel zone.¹¹ Figure 4b shows the received signal waveforms when a subject sits in a good versus a bad location for respiration detection in the Fresnel zone. Without loss of generality, within each Fresnel zone, the worst human location for centimeter-level subtle motion sensing is around the boundary, while the best location appears in the middle.

Leveraging multifrequency Fresnel zones to enhance respiration sensing. Consider the 30 subcarriers in the Intel 5300 Wi-Fi card with different wavelengths. According to P5, the Fresnel zone boundaries of all subcarriers almost overlap in the inner Fresnel zones; if one subcarrier cannot measure human respiration due to the person's poor location, the other subcarriers cannot either. But starting

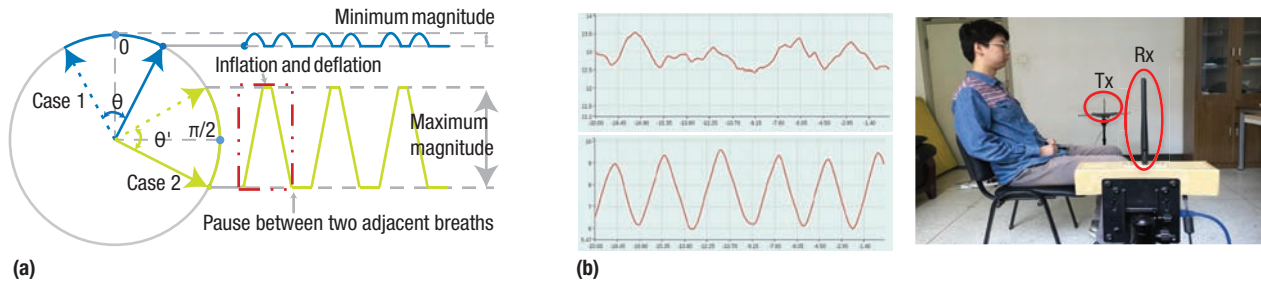


FIGURE 4. The received signal waveforms based on different human locations for (a) analytical versus (b) actual implementation.

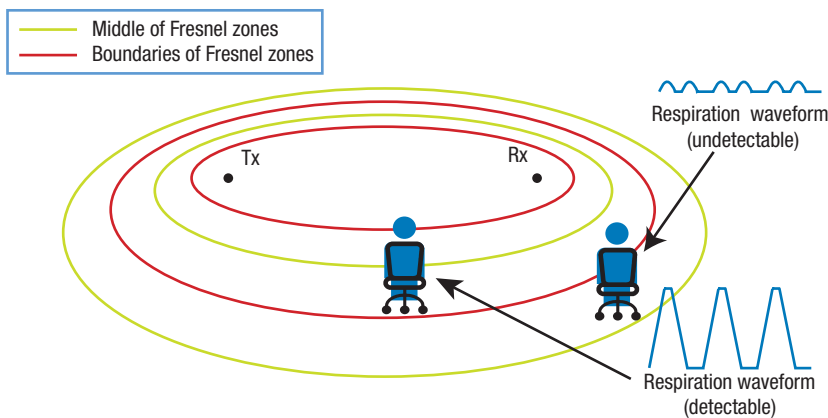


FIGURE 5. Our respiration detection map with respect to human location.

from a certain Fresnel zone outward, when the location is near a bad position (close to the Fresnel zone boundary) for one subcarrier, we can often exploit the frequency diversity to find another subcarrier showing a well-received signal waveform for the same position (near the middle of the Fresnel zone; see Figure 3c). With this observation in mind, we conducted real respiration-detection experiments with two Wi-Fi transceivers 70 cm apart (see Figure 4b) and found that from the 48th Fresnel zone onward, at least one subcarrier can locate the person in the middle of one Fresnel zone.¹¹ Without loss of generality, for subtle centimeter-scale human motion sensing, the frequency diversity can be exploited to enhance sensing in the outer Fresnel zones but not the inner Fresnel zones.

Respiration detection map with respect to human location. Our respiration-detection evaluation (see Figure 5) had three main results. First, the closer the person was to the Tx or Rx, the stronger the reflected CSI signals we obtained. When the person went beyond a zone limit (detection bound), no clear reflected CSI signals were received for accurate respiration detection. Second, in the region that was within but close to the detection bound—what we're calling the frequency diversity-enabled region—there was always one subcarrier that could sense human respiration

well. Third, in the inner Fresnel zones, we observed clear respiration waveforms when the subject was located in the middle of one zone, but this signal became increasingly distorted as the subject moved toward the Fresnel zone boundary until finally no clear signal was present.

Discussion. For micro human motions such as respiration-related chest movements, the reflected signal path length changes within the range of a wavelength. In this case, whether the micro motion is detectable or not depends not only on how strong the reflected signal

strength is compared to the direct signal strength but also on the location of the human body with respect to the two transceivers. Generally speaking, for a moving body that has a big reflective surface and is close to the LoS—which would generate a stronger reflected signal—if the motion is small but the location is ideal, the micro motion will still be accurately captured and detected. On the contrary, if the human motion cannot produce sufficient reflected signal strength in the receiver due to poor location, small reflective surface, or distance, even decimeter-scale human activities cannot be captured and detected well. Using the Fresnel zone model and signal superimposition equations, we can evaluate and inform the human activity recognition feasibility.

Estimation of indoor walking direction

Determining human walking direction in an indoor environment is important for many applications, from emergency evacuation and virtual reality to elderly care. Unfortunately, there is still no cost-effective solution that allows us to access this information continuously.

Walking direction in a 2D plane. Walking direction in a 2D plane could be easily determined if we knew the subject's precise indoor location. However, after two decades

of research on indoor localization with commodity Wi-Fi devices, accurately sensing human location remains challenging. Although both device-based and device-free location sensing techniques using commodity Wi-Fi devices have been actively explored, the state-of-the-art approach achieves only submeter-level accuracy,^{14,15} which is too coarse to derive accurate moving direction directly. In our recent work, we applied the Fresnel zone model to human indoor walking direction and distance estimation.¹²

Indoor walking direction can be defined in a 2D Cartesian coordinate system. Assume a person moves from point a to point b in the Cartesian coordinate plane, as shown in Figure 6; our goal is to estimate the angle of \vec{ab} . Assume that a pair of Tx-Rx1 devices are placed on the x-axis and a pair of Tx-Rx2 devices are placed on the y-axis, and then two sets of Fresnel zones are formed around the x- and y-axes. The solution to the direction-estimation problem is to find the direction of movement and distance in each coordinate in the context of Fresnel zones. As Figure 6 shows, the vector \vec{ab} can be decomposed into two subvectors \vec{ab}_x and \vec{ab}_y , where each subvector is parallel to one axis of the coordinate system. We then turn the \vec{ab} direction-estimation problem into the estimation of two subvectors \vec{ab}_x and \vec{ab}_y , separately, in terms of distance and direction in the corresponding Fresnel zones.

Subvector distance estimation. When a person crosses the Fresnel zones, he or she will generate peaks and valleys, with the number corresponding to the number of Fresnel zones crossed. The distance in the Fresnel zones can thus be expressed as the number of Fresnel zone boundaries crossed. According to property P2, the number of Fresnel zones crossed can be measured by counting the peaks and valleys of the received signal using fast Fourier transform;¹² this approach is quite accurate, especially when the moving direction is perpendicular to the Tx-Rx LoS.

Subvector direction estimation. Direction information for a certain Fresnel zone can be revealed by inspecting the relationship of Fresnel zones from multiple subcarriers. According to P7, the location of each Fresnel zone boundary from two subcarriers differs; thus, when a person walks in the Fresnel zones, he or she will cross the boundaries of Fresnel zones of different subcarriers sequentially.

To shed more light on this, consider a person moving inwardly through the Fresnel zones. Assume the wavelength of subcarrier 1 is longer than subcarrier 2. Because

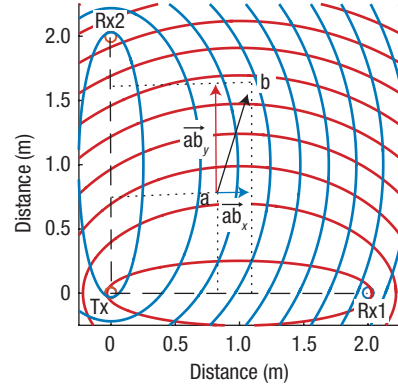


FIGURE 6. Indoor walking direction can be estimated on a 2D Cartesian coordinate system by finding the direction and distance moved in each coordinate in the context of the Fresnel zones.

the length of the reflected path is the same for both subcarriers, the initial Fresnel phase of subcarrier 1 is smaller. As the person keeps walking inwardly and crossing Fresnel zone boundaries, the length of the reflected path gets shorter and the Fresnel phase θ decreases and rotates clockwise; the two subcarriers' waveforms thus have a time delay Δt caused by the difference of each initial Fresnel phase θ . Therefore, we expect the waveform of subcarrier 1 to lead subcarrier 2. On the contrary, if the person moves outwardly through the Fresnel zones, its reflected path length increases and its Fresnel phase rotates counterclockwise. In this case, the waveform of subcarrier 2 leads subcarrier 1. By using a method to extract this precedence relationship among subcarriers, we are able to tell whether the person is moving inward or outward relative to a pair of Rx-Tx devices. This is the basic manner in which we extract direction information from Fresnel zones.

Discussion. We conducted an experiment in which subjects walked in eight directions in three different rooms: A, an empty room, and B and C, furnished office rooms of different sizes. Our prototype system achieved a median absolute error of 10° for direction estimation with three Wi-Fi devices, as shown in Figure 7; this is comparable to results with wearable sensor-based solutions.

The distance of macro human motion, such as walking, is much larger than a wavelength. In this case, all subcarriers generate signal fluctuations with precedence relationships. The walking direction estimation shows that decimeter-scale human motion can be sensed using a multi-frequency Fresnel zone model by correlating CSI waveforms of different subcarriers.¹² Apparently, when human motion crosses multiple Fresnel zones, deliberately placing more Wi-Fi receivers or antennas and creating several overlapped Fresnel zones allows both the direction and cycle number

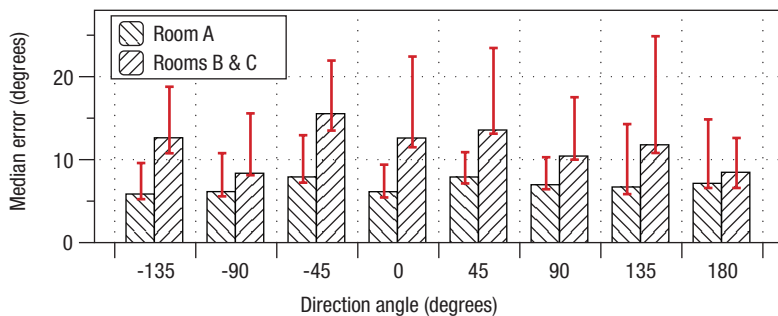


FIGURE 7. Our prototype system achieved a median absolute of 10° for direction estimation with three Wi-Fi devices for subjects walking in eight directions in an empty room (A) and furnished offices of different sizes (B and C).

ABOUT THE AUTHORS


DAQING ZHANG is a chair professor in the School of Electronics Engineering and Computer Science at Peking University. His research interests include context-aware computing, urban computing, mobile computing, big data analytics, and pervasive elderly care. Zhang received a PhD in electrical engineering from the University of Rome La Sapienza. He is the associate editor of *ACM Transactions on Intelligent Systems and Technology* and *IEEE Transactions on Big Data*. Contact him at dqzhang@sei.pku.edu.cn.

HAO WANG is a PhD student in computer science in the School of Electronics Engineering and Computer Science at Peking University. His research interests include mobile crowdsensing and ubiquitous computing. Wang received an MS in software engineering from the School of Software and Microelectronics at Peking University. Contact him at wanghao@sei.pku.edu.cn.

DAN WU is a PhD student in computer science in the School of Electronics Engineering and Computer Science at Peking University. His research interests include software modeling and ubiquitous computing. Wu received a BS in computer science from the University of Science and Technology of Beijing. Contact him at wudan@pku.edu.cn.

in different zones to be used as context information for recognizing or estimating macro human activities.

The Fresnel zone model is a new theoretical foundation for non-intrusive, contactless sensing using RF signals in indoor environments. This model not only explains the wavelength-scale signal fluctuation that human movement causes in each subcarrier at Wi-Fi receiver devices, but it also sheds light on the scale of human activities that can be sensed and recognized using Wi-Fi CSI—that is, Wi-Fi RF signals’ possible sensing limit. Building on the Fresnel zone model and Wi-Fi devices’ frequency diversity, centimeter-scale human activities such as respiration (micro) and decimeter-scale activities such as walking (macro) have been detected with high accuracy.

We have only scratched the surface of the Fresnel zone model’s possibilities. As our understanding of the model and the RF signal-propagation theory evolve, their role in wireless sensing will expand. In the shorter term, we envision the proposed theory accelerating the nonintrusive human-sensing field, enabling a wide spectrum of new applications in homes, offices, hospitals, warehouses, and more. In the longer term, we believe that synergizing communication and sensing capabilities in computing devices will fuel a revolution in both Internet of Things (IoT) and context-aware computing, which could result in wirelessly sensed big data and could expose sensed information about the environment and user behavior to future IoT architectures, enabling services that touch our everyday lives. 

ACKNOWLEDGMENTS

This work is supported by China's National Key Research and Development Plan (grant 2016YFB1001200) and Peking University's Key Discipline Construction Grant.

REFERENCES

1. Z. Yang, Z. Zhou, and Y. Liu, "From RSSI to CSI: Indoor Localization via Channel Response," *ACM Computing Surveys*, vol. 46, no. 2, 2013, p. 25.
2. D. Halperin et al., "Tool Release: Gathering 802.11n Traces with Channel State Information," *ACM SIGCOMM Computer Communication Rev.*, vol. 41, no. 1, 2011, p. 53.
3. H. Wang et al., "RT-Fall: A Real-time and Contactless Fall Detection System with Commodity WiFi Devices," *IEEE Trans. Mobile Computing*, vol. PP, no. 99, 2016; doi:10.1109/TMC.2016.2557795.
4. X. Liu et al., "Wi-Sleep: Contactless Sleep Monitoring via WiFi Signals," *Proc. IEEE Real-Time Systems Symp. (RTSS 14)*, 2014, pp. 346–355.
5. J. Liu et al., "Tracking Vital Signs During Sleep Leveraging Off-the-Shelf WiFi," *Proc. 16th ACM Int'l Symp. Mobile Ad Hoc Networking and Computing (MobiHoc 15)*, 2015, pp. 267–276.
6. C. Han et al., "WiFall: Device-Free Fall Detection by Wireless Networks," *Proc. IEEE Conf. Computer Communications (INFOCOM 14)*, 2014, pp. 271–279.
7. D. Tse and P. Viswanath, *Fundamentals of Wireless Communication*, Cambridge Univ. Press, 2005.
8. R. Nandakumar, B. Kellogg, and S. Gollakota, "Wi-Fi Gesture Recognition on Existing Devices," arXiv, 19 Nov. 2014; arXiv:1411.5394.
9. W. Wang et al., "Understanding and Modeling of WiFi Signal Based Human Activity Recognition," *Proc. 21st ACM Ann. Int'l Conf. Mobile Computing and Networking (MobiCom 15)*, 2015, pp. 65–76.
10. H.D. Hristov, *Fresnel Zones in Wireless Links, Zone Plate Lenses and Antennas*, Artech House, 2010.
11. H. Wang et al., "Human Respiration Detection with Commodity WiFi Devices: Do User Location and Body Orientation Matter?," *Proc. ACM Int'l Joint Conf. Pervasive and Ubiquitous Computing (UbiComp 16)*, 2016, pp. 25–36.
12. D. Wu et al., "WiDir: Walking Direction Estimation Using Wireless Signals," *Proc. ACM Int'l Joint Conf. Pervasive and Ubiquitous Computing (UbiComp 16)*, 2016, pp. 351–362.
13. C. Lowanichkiattikul et al., "Impact of Chest Wall Motion Caused by Respiration in Adjuvant Radiotherapy for Postoperative Breast Cancer Patients," *SpringerPlus*, vol. 5, 2016; doi:10.1186/s40064-016-1831-3.
14. M. Kotaru et al., "SpotFi: Decimeter Level Localization Using WiFi," *Proc. ACM Conf. Special Interest Group on Data Communication (SIGCOMM 15)*, 2015, pp. 269–282.
15. K. Qian et al., "Decimeter Level Passive Tracking with WiFi," *Proc. 3rd Workshop on Hot Topics in Wireless (HotWireless 16)*, 2016, pp. 44–48.



Are Enemy Hackers Slipping through Your Team's Defenses?

Protect Your Organization from Hackers by Thinking Like Them

Take Our E-Learning Courses in the Art of Hacking

You and your staff can take these courses where you are and at your own pace, getting hands-on, real-world training that you can put to work immediately.

www.computer.org/artofhacking

